International Journal of Rotating Machinery, 10(5): 387–399, 2004

ISSN: 1023-621X print / 1542-3034 online
DOI: 10.1080/10236210490474548

Taylor & Francis
Taylor & Francis Group

The Pre-Stall Behavior of a 4-Stage Transonic Compressor and Stall Monitoring Based on Artificial Neural Networks

Frank-Oliver Methling and Horst Stoff
Fluid Energy Machines, Ruhr-University Bochum, Germany

Frank Grauer
MTU Aero Engines, Munich, Germany

Current research concerned with the aerodynamic instability of compressors aims at an extension of the operating range of the compressor towards decreased massflow. In practice, a safety margin is maintained between operating point and stability limit to prevent the compressor from going into stall and surge. In this article, we analyze the behavior of a 4-stage transonic axial compressor before entering the unstable range and present an approach to identifying incipient surge and stall using artificial neural networks. This method is based on measurements of the unsteady static wall pressure in front of the first rotor.

Analyzing the static pressure signals by using the Fast Fourier Transform shows that peripheral disturbances (modal waves) can only be identified in a small range close to nominal speed (at 95%). At lower speeds (60 to 80% of nominal speed), the investigated compressor flow enters instability by spike-type stall.

Monitoring stability over the entire speed range of the compressor relies on artificial neural networks using the unsteady wall pressure signal. In the present case, artificial neural networks show to be the most useful tool to indicate approaching instability. The method works reliably for both types of instabilities, spike-type stall as well as modal waves.

Keywords Axial compressor, Rotating Stall, Surge, Pre-stall behavior, Fourier analysis, Artificial neural networks

INTRODUCTION

In a compressor performance map the surge line is the limit of aerodynamic stability towards low massflow. The different forms of those aerodynamic instabilities are rotating stall and surge. Rotating stall defines a situation where regions of reversed flow occur locally. Surge is characterized by a system instability with periodic backflow over the entire cross section involving violent oscillations in the ducts and piping throughout the compression system. Surge can be divided into two different forms: the so-called *classic surge* when the mass flow decreases intermittently, and *deep surge* in which the mass flow becomes negative. The different forms are described in detail by Day (1996a) and Rippl (1995).

Figure 1 shows the schematic view of the performance map of a compressor for the purpose of discussing forms of instability.

All of those forms of instability are stressing the engine heavily, and may lead to mechanical failure. Strain gauge measurements in the literature report of bending stress in vanes exceeding stable operation by a factor of two during surge and by five under conditions of rotating stall (Rippl, 1995). For this reason, numerous investigations are under way to find reliable means for monitoring an eventual approach to the stability limit while running the machine (Ludwig and Nenni, 1978; Day et al., 1997; Höss et al., 1998; Walbaum and Rieß, 1998). Ways for alerts have been identified for individual test beds but a reliable warning of general validity also for foreign compressor designs is still unattained (Ludwig and Nenni, 1980; Schulze et al., 1998; Regnery, 1998; Grauer, 1998a, b), therefore the quest for proof of reliability initiates additional research. Different concepts have

Received 25 June 2002; accepted 1 July 2002.

The stall measurements on the compressor rig were carried out at the University of Hannover, Institut für Strömungsmaschinen. The data analysis at the University of Bochum were supported by the German Ministry of Education and Research (BMBF) together with MTU during the project "AG TURBO II" under grant no. 0327061 J/9. We gratefully acknowledge all these contributions.

Address correspondence to Frank-Oliver Methling, Fluid Energy Machines, Ruhr-University Bochum, 1B4-142, Universitatsstr. 150, Bochum, D-44801, Germany. E-mail: methling@methling.com

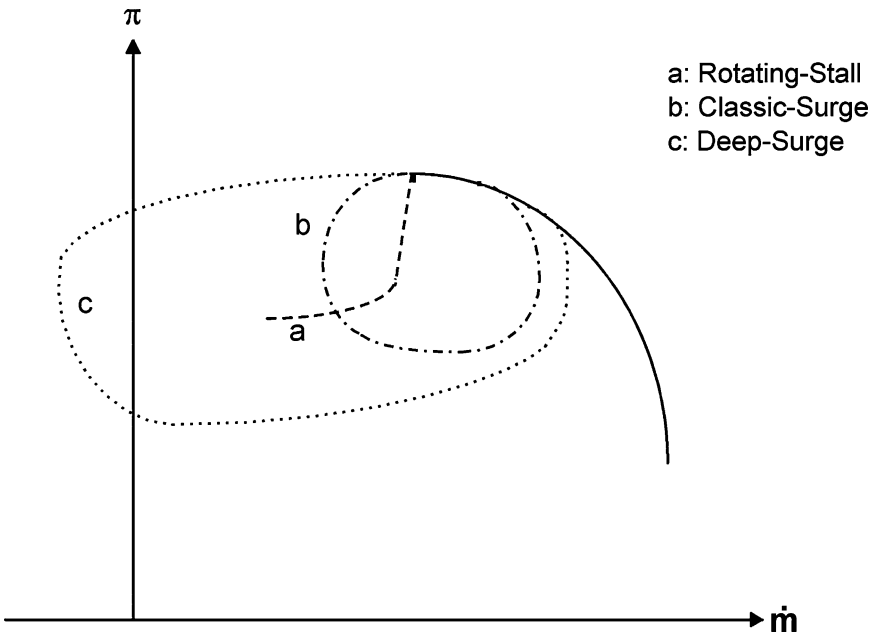

FIGURE 1
Compressor performance during stall and surge.

been devised to prevent the compressor from entering unstable operation by increasing the distance to the surge line as soon as a critical approach is detected. This may be done by opening blow-off valves, adjusting guide vanes, or reducing fuel in gas turbines. Another concept describes attempts to move the surge line actively towards lower throughflow and higher pressures by the influence of actuators, e.g., the "modal" control (Murray, 2001) with pulsed air injection. Doing this enables the maintaining of the speed line and the shifting of the surge line to provide for increased operating range (Day, 1996b; Paduano, 2000). No matter what the approach to avoid stall and surge will be, however, it is first necessary to detect upcoming unstable conditions reliably.

The following sections present investigations about the onset of rotating stall in a high-speed axial compressor of 4 stages by using high resolution wall pressure measurements. Results of data analyses are presented that aim to deliver a reliable technique to detecting the approach to the unstable range.

EXPERIMENTAL SETUP

Compressor Test Rig

The 4-stage test compressor at the lab of the University of Hannover (Figure 2) is equipped with controlled diffusion airfoils (CDA). Its specifications are listed in Table 1.

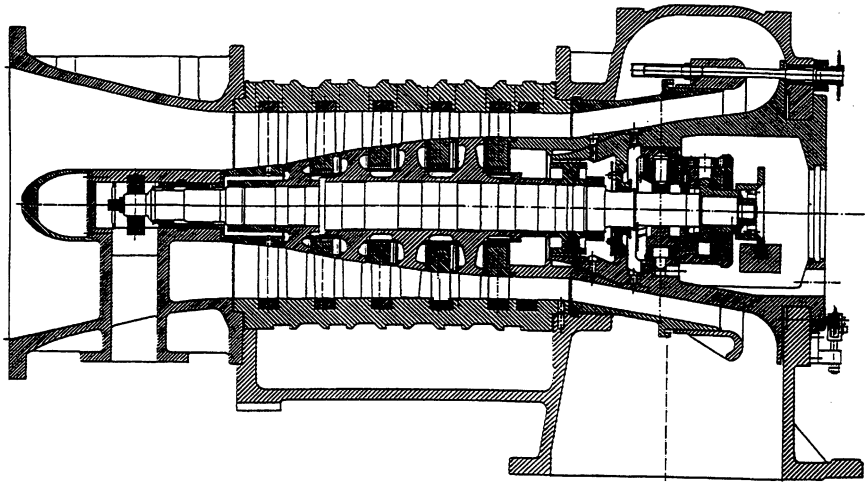

FIGURE 2
4-stage compressor.

TABLE 1
Compressor data

Nominal speed (100%)	18000 min^{-1}	Number of blades and vanes		
Corrected massflow	14,1 kg/s		IGV	26
Inlet pressure	0,5 . . . 1,0 bar	Stage 1	Rotor 1	23
Isentropic efficiency	0,88		Stator 1	30
Pressure ratio	2,95	Stage 2	Rotor 2	27
No. of stages	4		Stator 2	32
Tip diameter (const.)	340 mm	Stage 3	Rotor 3	28
Blade height	90 . . . 45 mm		Stator 3	34
Axial velocity	189 . . . 150 m/s	Stage 4	Rotor 4	31
Circumferential velocity	320 m/s		Stator 4	36

The compressor inlet mass flow can be throttled to limit the power consumption and blade stresses. All tests are taken with an inlet pressure of 0.6 bar. The instability is caused by throttling downstream. Due to the downstream volume enclosed by the throttle, the compressor even remains in rotating stall as a steady-state operation without going into surge, independent of the compressor speed.

Instrumentation

Unsteady flow data are acquired from wall-mounted probes for static-pressure. Figure 3 shows the circumferential positions of pressure probes in front of the first rotor. At position "3" (162°), the probe is positioned behind the first blade row. Another sensor (not given in Figure 3) is positioned above the blading of the first rotor. In axial direction one probe is mounted in front of each cascade at position "4" (255°) (see Figure 3 (right)).

The pressure transducers enable the resolving of very high frequencies. All measurements that are presented here were taken at a sampling rate of 50 kHz with a low pass filter of 20 kHz corresponding to the Nyquist criterion.

Database

The performance map of the compressor and the database for the analysis is given in Figure 4.

The investigations mentioned here are based on two independent tests for each marked operating point to compare the results.

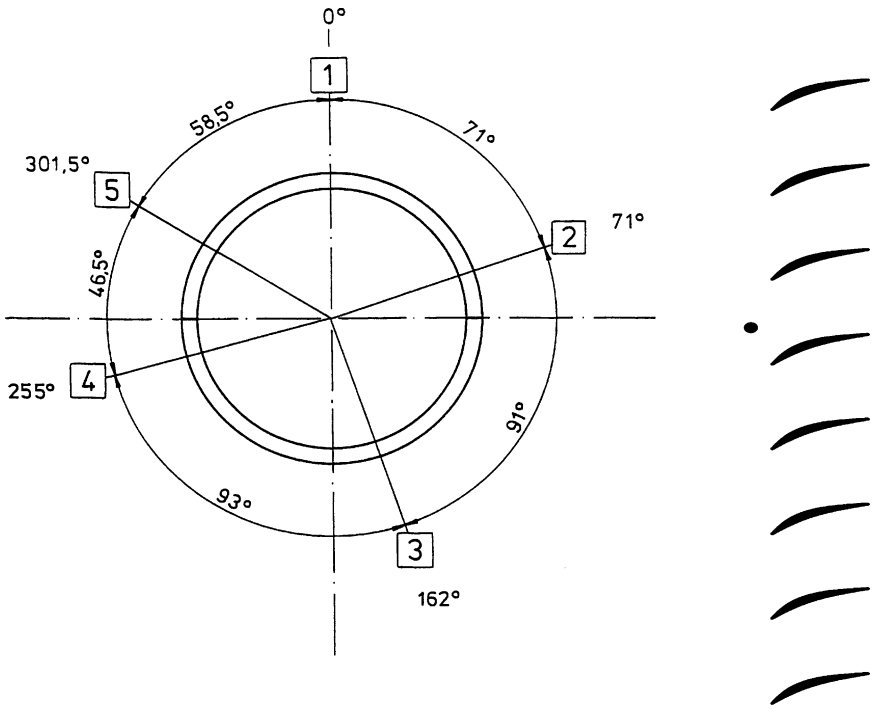

FIGURE 3
Circumferential (left) and axial (right) positions of pressure probes in front of the first rotor of flow.

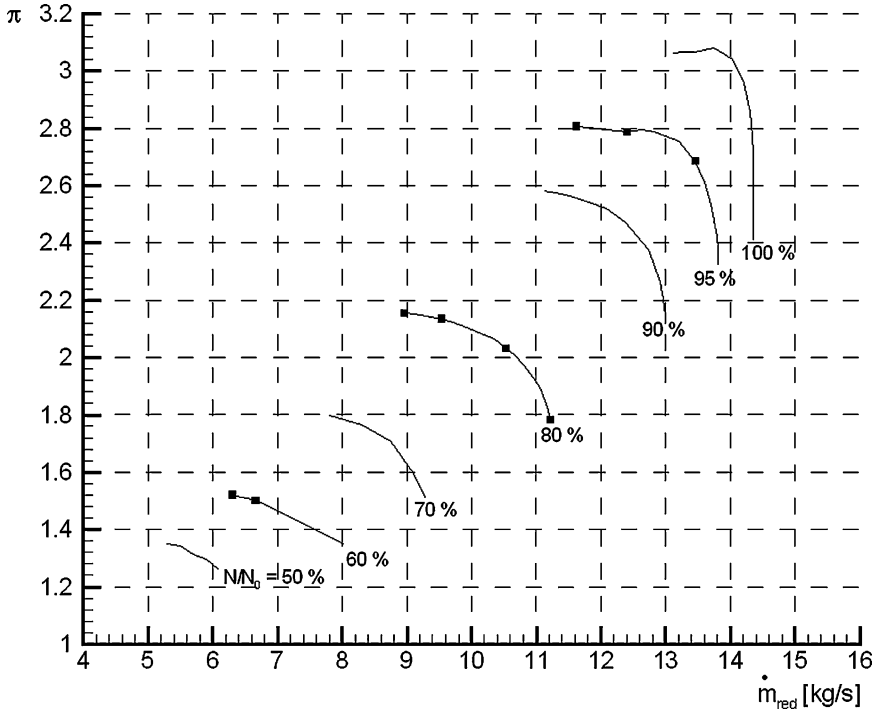

FIGURE 4
Compressor performance map and database.

The static pressure was recorded at the different circumferential positions referred to before: four in front of rotor 1, one above rotor 1, and one in front of each rotor and stator as shown in Figure 3. The results of the analysis are given in the following sections.

RESULTS OF UNSTEADY MEASUREMENTS

The unsteady behavior of the compressor was measured at the relative speeds of 60%, 80% and 95%. The instability was introduced by downstream throttling. At each compressor speed the instability started at the front end of the compressor, i.e., the

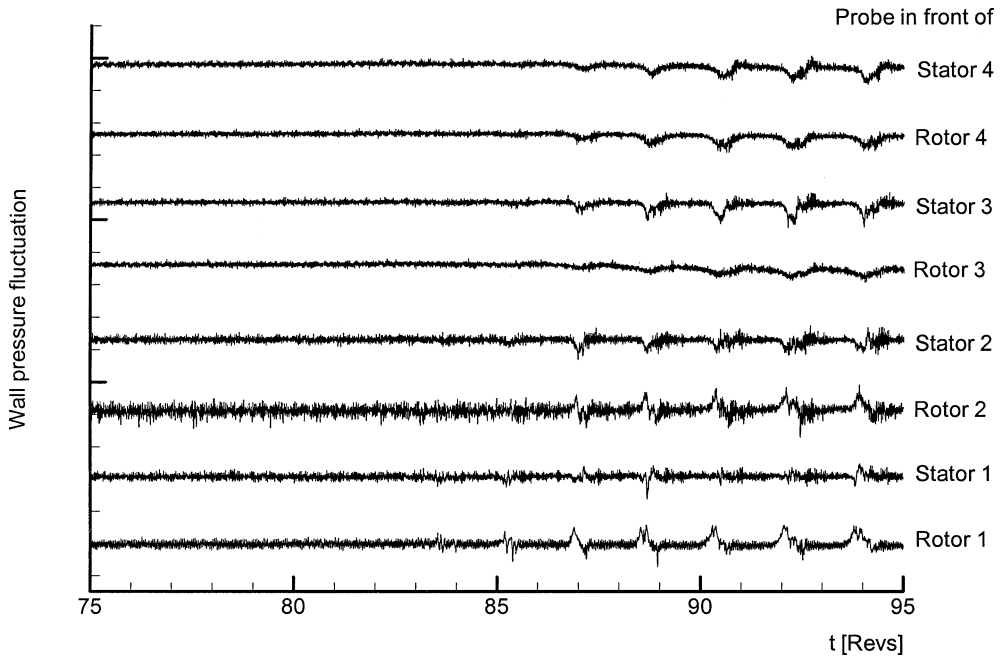

FIGURE 5
Distribution of wall pressure at different axial positions vs. time (revs) at 60% of nominal rotor speed.

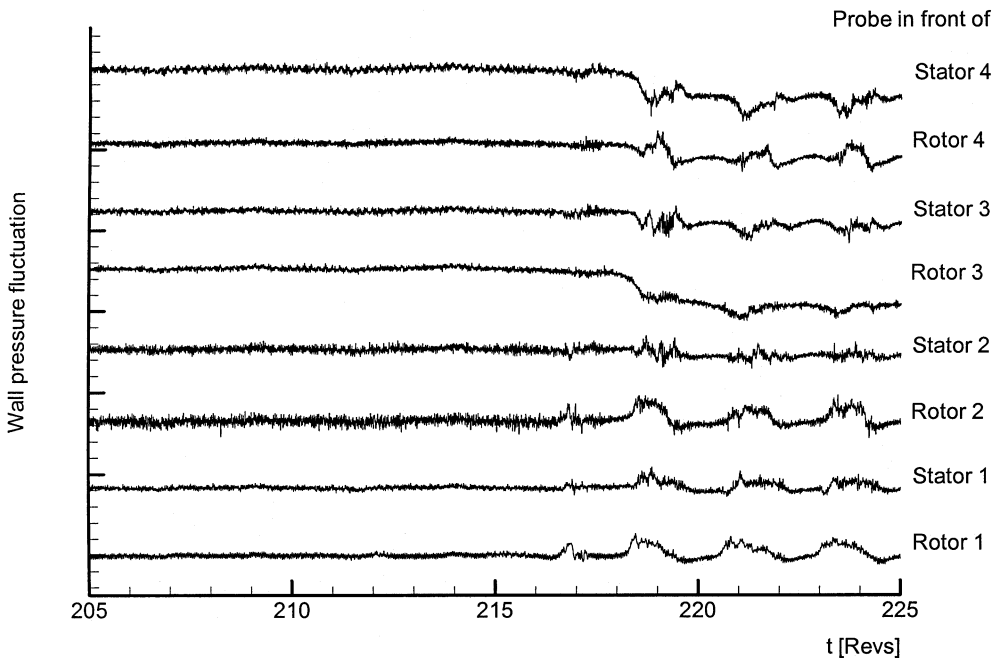

FIGURE 6
Distribution of wall pressure at different axial positions vs. time (revs) at 80% of nominal rotor speed.

probes in stages #1 and #2 detected the emerging spike first (see Figures 5–7).

Figure 8 shows the signals as acquired from the measurement beginning about four revolutions ahead of the stall event. The rotational speed of the emerging spike is about 54% of the rotor speed when going into rotating stall. The rotating stall is of the type of a one-cell configuration with a rotational speed of 43.5% of the blade speed.

When approaching the situation of stall, it is not easily possible to recognize the appearance of precursor wave patterns at a

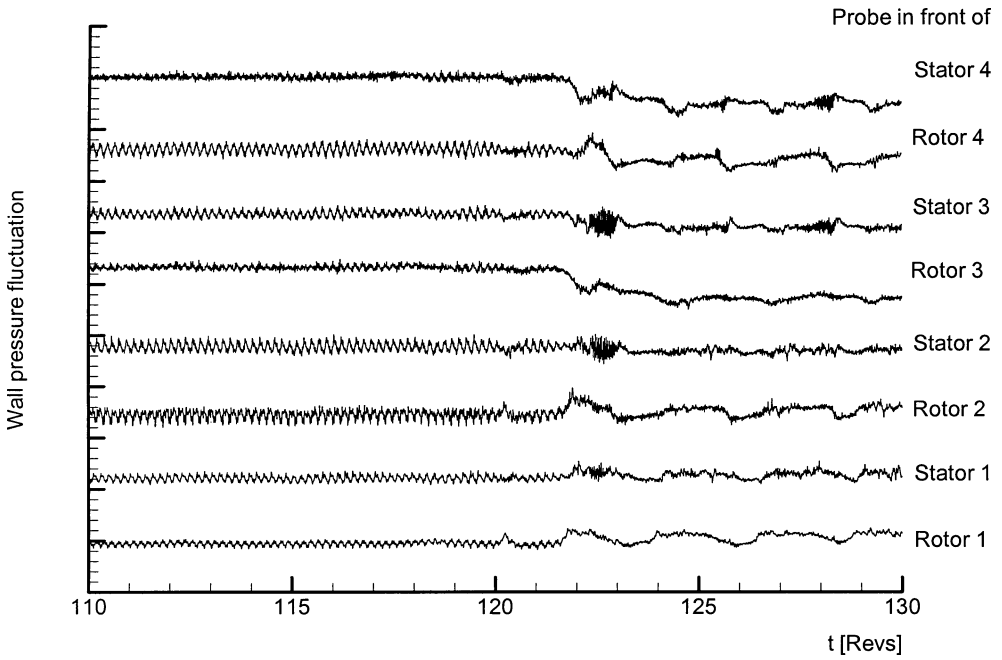

FIGURE 7
Distribution of wall pressure at different axial positions vs. time (revs) at 95% of nominal rotor speed.

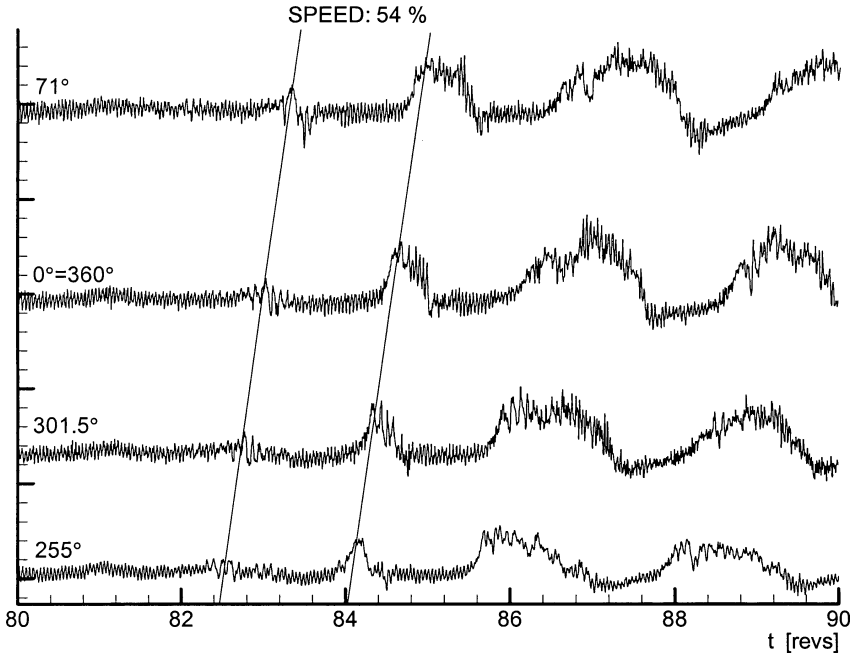

FIGURE 8
Distribution of wall pressure at different circumferential positions in front of rotor #1 vs. time (revs) at 80% of nominal rotor speed.

time sufficiently large to allow for preventive action. The emerging spike increases to stall within less than two revolutions. A precursor wave information serving as a stall detector cannot be discerned sufficiently early.

Precursors such as modal waves cannot be detected from the measured data without any further analysis. As mentioned above, first it is necessary to detect the approach of the compressor operating condition to the unstable range before developing a control system to avoid this. Therefore, different methods of analyses were developed and tested at the University of Bochum which aim at a reliable detection of reaching the unstable range of the compressor performance map.

RESULTS OF THE DATA ANALYSIS

The Fourier transform of a signal provides information about the amplitudes of different oscillations with respect to the rotor revolutions. Due to the different types of stall inception described, for example, by Day, 1996a in which modal waves are as large-scale disturbances and spikes as short-scale disturbances, the Fourier transform is able to identify those disturbances in their band of frequency relative to the rotor speed.

In this article only the results of Fourier transforms of single sensor signals will be given. The analyzed data was acquired by a sensor ahead of the first rotor. Another technique first described by Tryfonidis (1994) is not used here because of the sensor positions. The circumferential Fourier transform uses evenly spaced pressure transducers. In this case only a sector of 176° of the circumference is covered by 4 sensors. Due to these peripheral positions, a circumferential Fourier transform will deliver incorrect results because of aliasing effects.

The results of the Fourier transform of a single sensor signal are given for the different compressor speeds in Figures 9 (60%), 10 (80%), and 11 (95%) over a time of 500 revolutions prior to instability. In the lower part of each figure the frequency vs. time (revs) and the amplitude (contour) are displayed; in the upper part, the integration of amplitudes in the frequency range of 0.1 to 1.0 is given. Former investigations have shown that it might be possible to detect the approach of a compression system to unstable conditions by observing the integration of amplitudes over a defined band of frequencies at one instant of time (Grauer, 1998a; Methling, 2000).

At 60 and 80% compressor speed, there are no frequency ranges where the amplitudes grow when the working line approaches the stability limit. At 60% (Figure 9), the sensor signal is noisy over the whole range of frequencies between 0 and 100% of rotor frequency. The signal of the 80% relative compressor speed (Figure 10) is very noisy in a range from 0 to 35% of the rotor frequency, but there is no range of an increasing amplitude.

Another result can be observed from the measurements at 95% rotor speed (Figure 11). At the frequency band less than 25% of the rotor frequency, the amplitudes grow when the working line approaches the stability limit. The integration of amplitudes begins to increase 120 revolutions prior to stall. The results of this analysis show, that only for the compressor speed of 95%,

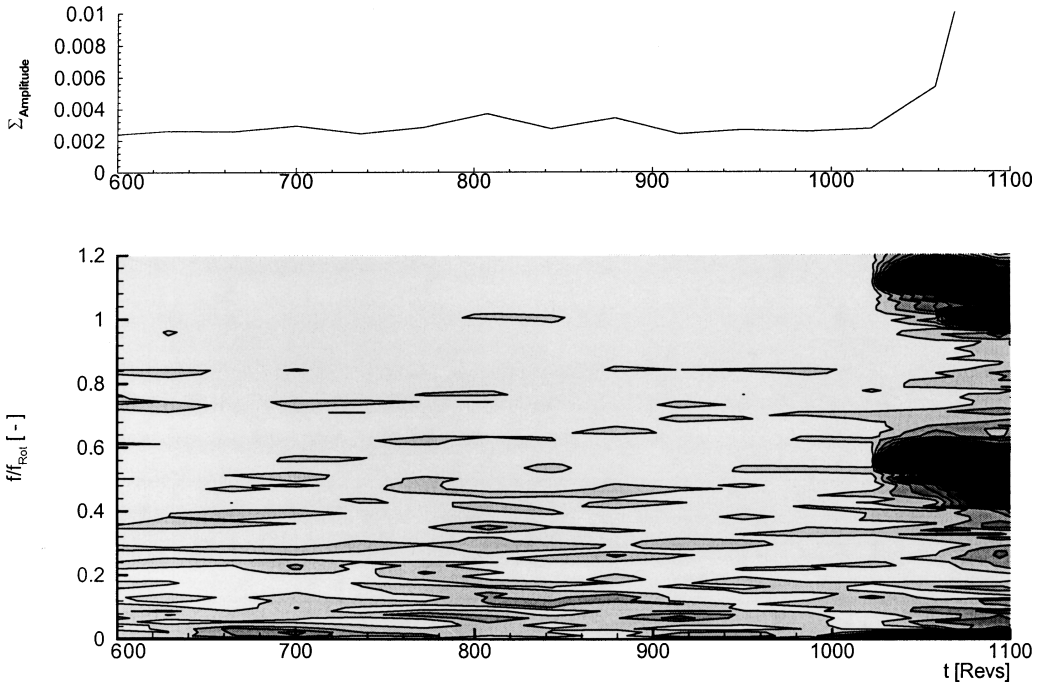

FIGURE 9
Fourier transform at 60% speed.

there exist frequency ranges where the amplitudes grow gradually prior to unstable conditions.

A criterion for a stall warning cannot be figured out by observing a special frequency or integrating the amplitudes within a frequency band in the case of this compressor.

As well as it is impossible to use this analysis as a precursor detection, it is impossible to identify the stable operation of the compressor from operation near the surge line (see Figure 12).

Figure 12 displays the integration of amplitudes at the last stable operating point (see Figure 4) at left and over a range of

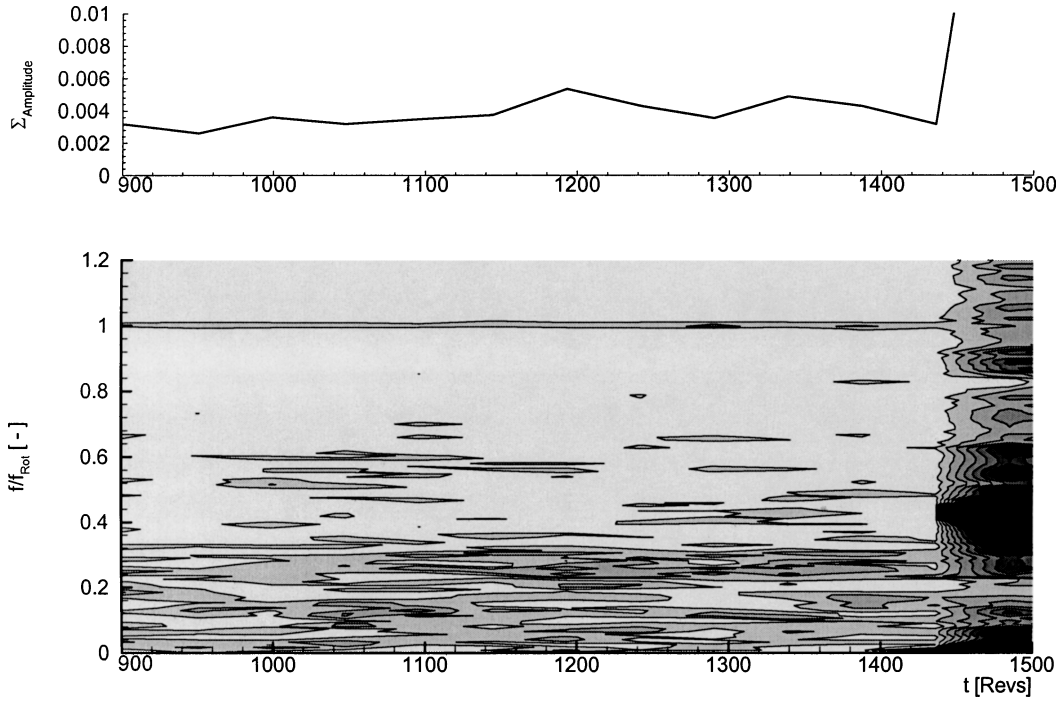

FIGURE 10
Fourier transform at 80% speed.

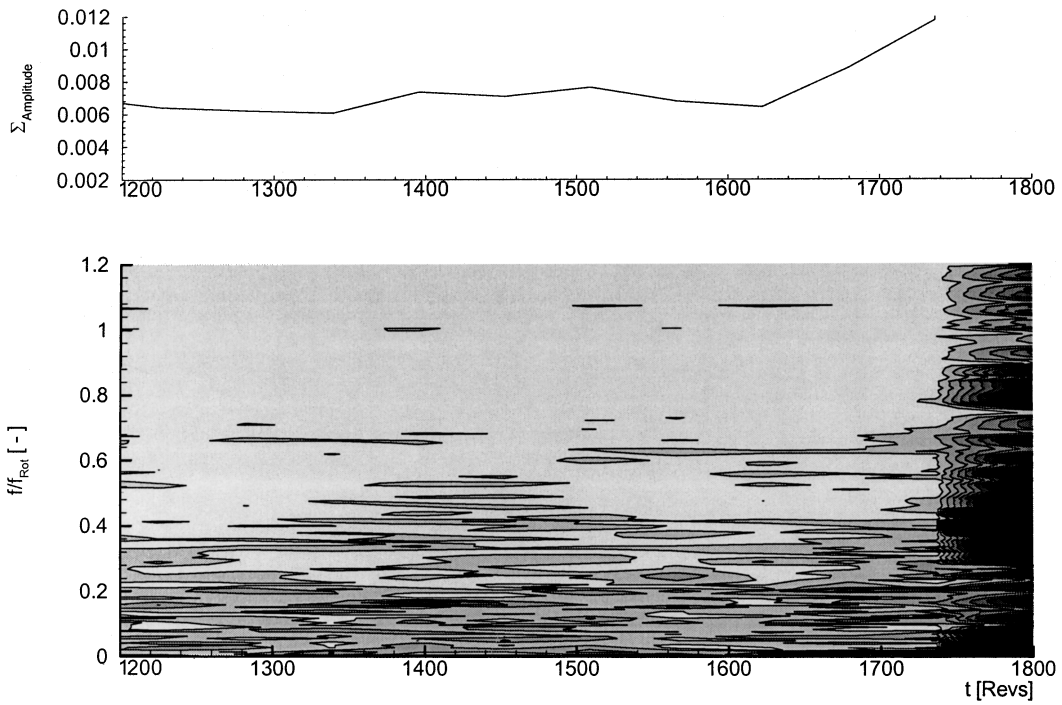

FIGURE 11
Fourier transform at 95% speed.

75 revolutions prior to stall at right for the different compressor speeds of 60% (top), 80% (middle), and 95% (bottom).

The result given in Figure 12 is the sum of amplitudes calculated by the Fourier transform at each timestep in the frequency band between $f/f_{Rot} = 0.1$ and 1.0.

In the upper speed ranges (80 and 95%) of the compressor, the integrated amplitudes show a higher level and an increase of fluctuations near the stability limit compared to the stable operation. At 60% compressor speed a distinction is impossible.

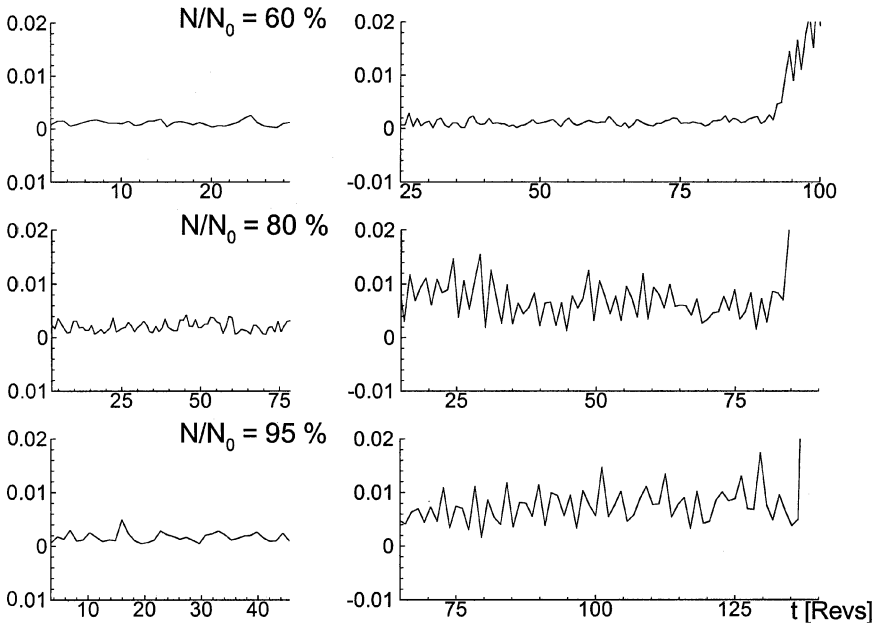

FIGURE 12
Comparison of integrated amplitudes at stable conditions (left) and near stall (right).

The described signal treatment cannot easily yield a criterion for a stall warning, but they give a deeper insight into the characteristics of the signal during the stall inception process. Another technique, which centers on the observation of the disturbances specific for the rotor speed, is based on artificial neural networks. This technique was first described by Grauer (1998a, b) and was adjusted to the present set of data as described in the following section.

MONITORING BASED ON NEURAL NETWORKS

Artificial neural networks attempt to imitate the biological brain in technical applications as there are the fields of pattern recognition and control. They can be adapted to a variety of problems and are able to extract information submerged in noise of a signal. Their capability goes beyond a simple analysis of the data as they can also serve for purposes of control. Figure 13 shows the basic elements of a neural network.

A neural network consists of many nonlinear computational elements called nodes (represented by rectangles in Figure 13) which are connected by links of variable weights. Data that have to be processed by the network reach the net via an input layer and are transmitted to the following layers by the weighted links. Basics about neural networks can be found in the literature (e.g., Ritter et al., 1991; Zell, 1994). Working with a neural network requires initial adaptation of the net to the special problem. This is done during a separate process called the learning or training phase. One of the methods most frequently used is called *supervised learning*, which means that representative data, which describe the problem as detailed as possible, are presented to the net together with the respective output. The learning process is finished, if the calculated error between the network output and the teaching output reaches a prescribed tolerance margin.

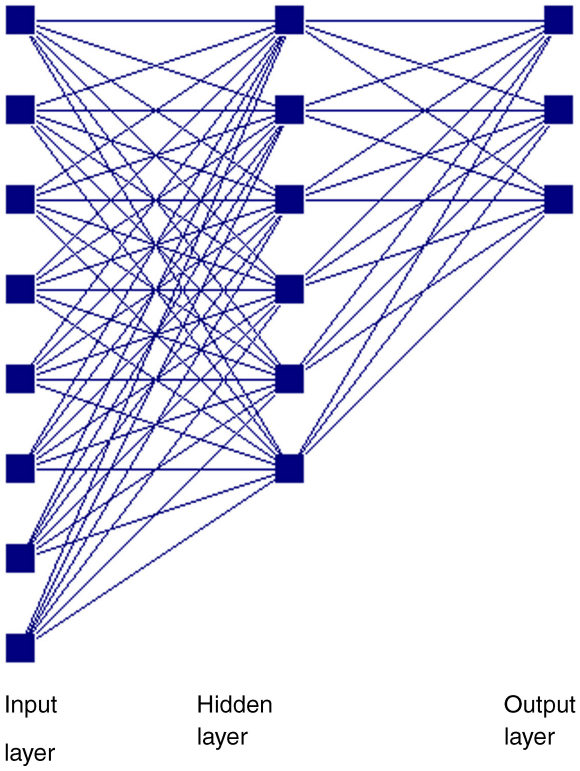

FIGURE 13
Basic elements of neural networks.

The results presented were obtained by the Stuttgart Neural Network Simulator (SNNS) which is developed at the Institute for Parallel and Distributed High Performance Systems (IPVR) of the University of Stuttgart, Germany. The simulator consists of various types of networks and a huge number of specific parameters. In the following, a feedforward net and the cascade correlation learning algorithm was used (Zell, 1994), as this combination yielded the best results.

Each neural network will work as well as the data, which were presented during the learning period, to describe the problem to be handled. Therefore, apart from a good choice of network models, connection types, and learning rules, which all have a significant influence on the network's performance, the most important step is to extract adequate sets of data (called *input pattern*). Measured data can be improved by appropriate preprocessing, which can be achieved by various analysis techniques. As described in the former section, different periodic disturbances and increasing fluctuations were found in the pressure signal that changed during stall inception.

Several analysis techniques gave insight into the structure of the pressure fluctuations. Referring to Figure 10, the distinction between stable operation and those operating points near stall was clearly indicated for example by the Fourier transform followed by the integration of amplitudes for the 80 and 95% speed line but not at 60% speed as described in the former section. As these differences also should be visible in the untreated pressure signals, they were observed in detail to find out comparable structures. Furthermore, the possibility of finding a criterion that enables one to distinguish between stable operation on the one hand and operation near surge line on the other hand for all the different compressor speed lines should be investigated. As described above, this was not possible by an analysis technique using the Fourier transform, therefore the neural network approach was chosen as described in the following.

The input to the network was generated by using wall static pressure signals. These pressure signals show specific characteristics which can be related to the actual operating point by using a neural network. The generation of the input pattern for the training as well as for the validation of the neural network has been done in the following steps:

1. Treatment of the measurement data to achieve a sampling rate of 10 kHz, i.e., each rotor revolution is represented by 35 samples at 95% relative speed and up to 55 samples at 60% relative speed.
2. The once-per-rev signal was used to start the recording of each input pattern. The length of the generated pattern covers

an interval of 30 samples which means nearly one rotor revolution (depending on the rotor speed). By using the once-per-rev signal, the beginning of the record of each pattern always starts at the same relative rotor position, i.e., the same peripheral sector of a revolution for each pattern.

3. Each of these pressure patterns (= set of 30 samples) was then normalized into an interval of [0,1] for each throttle setting in order to level the signal by using (Equation 1).

$$\bar{p}(t) = \frac{p(t) - \min(p)}{\max(p) - \min(p)} \forall t \in [1; 30] \qquad [1]$$

applied to each pattern, i.e., revolution, where

$p(t)$ = measured value,

$\bar{p}(t)$ = normalized value,

max/min = maximum/minimum value of each pattern

The way of input pattern generation from the pressure signal is given in Figure 14. By using this way of pattern generation each rotor revolution yields one pressure signature for the network input. This approach was chosen because in some cases only few data for the network training were available and the pattern generation suggested by Grauer (1998b), which is based on an additional ensemble averaging of this single-rev pattern, would further reduce the available training data.

This generation of input pattern for the neural network has been done for all the selected speed lines of the compressor.

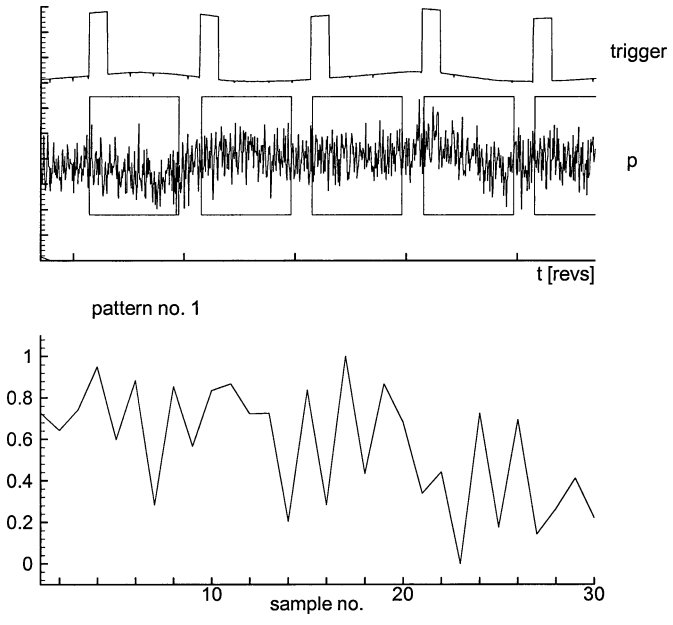

FIGURE 14
Generation of input pattern.

TABLE 2
Number of Pattern, i.e., Training Database

Nominal speed	Stable operation	Operation near surge line
60%	30	92
80%	237	82
95%	94	138

As mentioned above, the database includes two independent measurements at each operating point. The network was trained with the data of one sensor of the first campaign and was then tested with the signals of the same sensor of the second set of measurements. Table 2 provides the number of generated pattern (= number of measured revolutions) for each operating range used for the training of the neural network.

The network generated with those data is given in Figure 15.

The teaching output of the network was defined as 0.3 for regions of stable operation and as 1.0 for operating points that are approaching the surge line. Figures 16 to 18 display the results of data classification using the network shown above (Figure 15) with the "unknown" testdata put into the network.

Figures 16 to 18 show the averaged network output for each compressor speed. Each dataset consists of the pattern from the stable operating range as well as from a dataset approaching the surge line. As it can be seen, the network output does not exactly correspond to the teaching output (defined before as 0.3 or 1.0) but such an artificial neural network can clearly decide between stable and unstable compressor operation.

Due to the high-speed data acquisition of transient data, this behavior of the network output is expected and an averaging of the network output is necessary. In the case of the results given here, the network output was averaged over a number of ten sets of pattern.

It is impossible to eliminate all the fluctuations by ensemble averaging caused by the fluctuations in the signal. Nevertheless, the network output is unambiguous if the result is considered, e.g., by a decision as "less than 0.7" or "greater than 0.7", for the stable and unstable range.

By analyzing the averaged network output in this way it can be stated that with the exception of some input patterns at rated speed of 60% and one input pattern at rated speed of 95%, all input patterns are classified correctly, i.e., the system is highly reliable. In all cases the operation near the surge line is classified correctly. Due to the database given in Table 3, the quality of the provided results depends on the number and length of available measurements.

The described method centers on the observation of the disturbances being periodic with the rotor speed. Those disturbances can be found in compressors with a spike-type stall and in those with modal waves (Day et al., 1997). It should be possible to apply this method to both types of onset of instability. This will be a subject for future investigations.

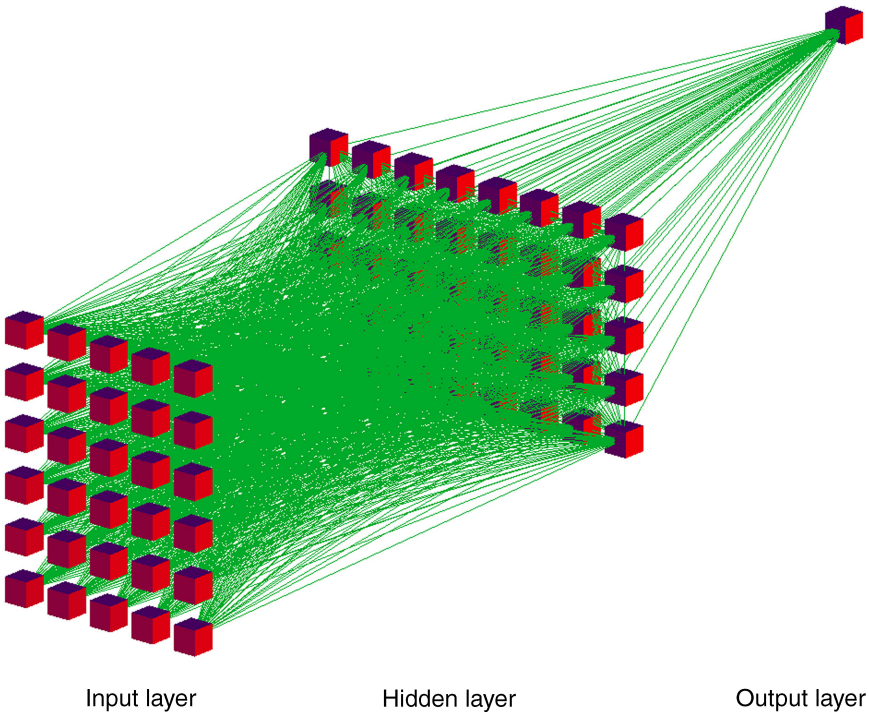

FIGURE 15
Neural network after training.

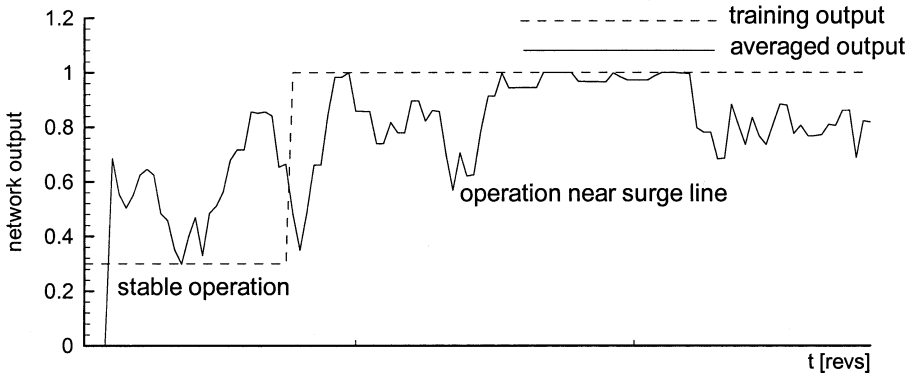

FIGURE 16
Network output, rotor speed 60%.

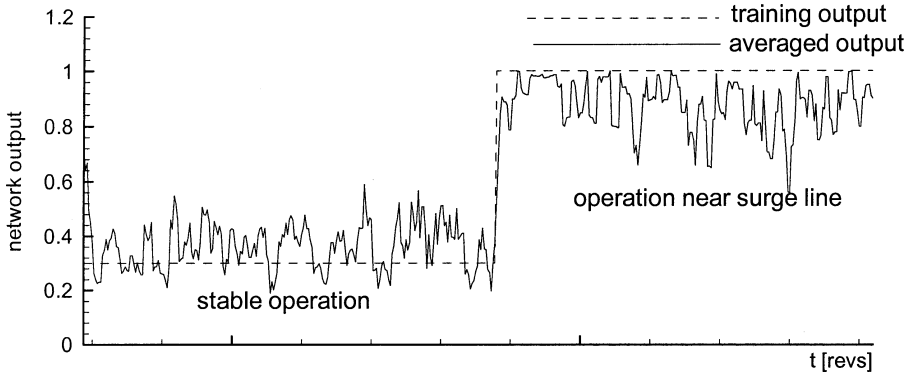

FIGURE 17
Network output, rotor speed 80%.

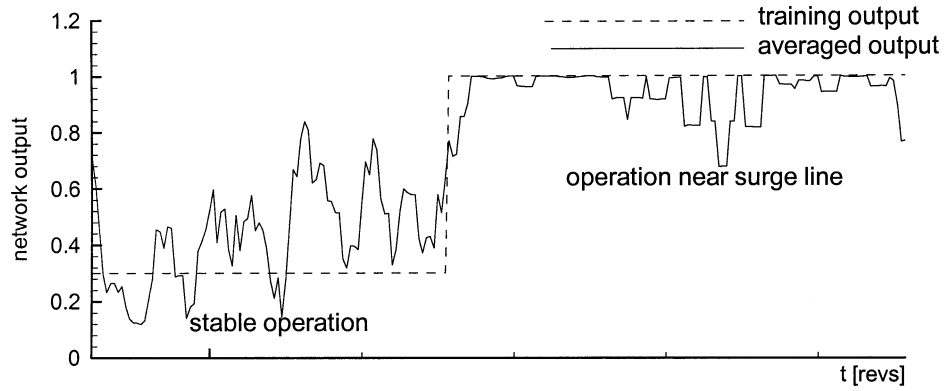

FIGURE 18
Network output, rotor speed 95%.

This and former investigations suggested that a monitoring system using neural networks could be useful. A disadvantage could be that each compressor type needs his "own" neural network and a measured database for the training of the network. The transfer of a network to another compressor of the same type is not yet investigated.

CONCLUSIONS

Unsteady measurements of wall pressures in the casing in front of each rotor and stator of the four stages and at the exit are considered in the investigations.

The inception of instability is of a spike-type stall. The rotational speed of the emerging spike is about 54% of the rotor speed going into stall with a single-cell configuration at a relative speed of 43% during a time of less than 2 rotor revolutions. In the case of 60 and 80% relative rotor speed, no precursor waves were detected. At 95% rotor speed the amplitudes in a frequency band up to 25% of the rotor speed begin to increase 120 revolutions prior to instability.

The integration of the amplitudes over the frequencies alone as a criterion for a stall warning is not able to cover the whole speed range. At 80 and 95% compressor speed there is a clear difference in variation and level of the integrated amplitudes. However, it is not possible at 60% speed to decide in this way between stable operation and an approach towards the surge line.

Artificial neural networks proved to be a useful tool to detect the actual compressor operation directly from the acquired data without any extensive preprocessing, i.e., deciding reliably between stable operation and operation near the surge line for all the different compressor speeds. The efficiency of this method depends on the availability of measured data to describe the technical problem. Consequently, the quality of the achieved results increased from 60% over 95% to 80% due to the number of available measurements at each compressor speedline. A monitoring system based on neural networks proved to be able to cover the whole range of the compressor operation if adequate training data are available.

REFERENCES

Day, I. J. 1996a. The fundamentals of stall and surge in axial compressors. *VKI Lecture Series 1996-05*, Unsteady Flow in Turbomachinery, Von Karman Institute for Fluid Dynamics Brussels, Rhode-St-Genese, Belgium.

Day, I. J. 1996b. Stall and surge in high speed compressors and the prospect for active control. *VKI Lecture Series 1996-05*, Unsteady Flow in Turbomachinery, Von Karman Institute for Fluid Dynamics Brussels, Rhode-St-Genese, Belgium.

Day, I. J. et al. 1997. Stall inception and the prospects for active control in four high speed compressors. *ASME 97-GT-281*, *Journal of Turbomachinery* 121(1):18–27.

Grauer, F. et al. 1998a. Detection of precursor waves announcing stall in two 3-stage axial compressors. *ASME 98-GT-520*.

Grauer, F. 1998b. Entwicklung einer pumpgrenzwarnung für mehrstufige, hochbelastete axialverdichter. *Fortschr.-Ber. VDI-Reihe 7 Nr. 355*.

Höss, B. et al. 1998. Stall inception in the compressor system of a turbofan engine. *ASME 98-GT-475*, *Journal of Turbomachinery* 122(1):32–44.

Ludwig, G. R., and Nenni, J. P. 1978. A Rotating stall control system for turbojet engines. *ASME 78-GT-115, Journal of Engineering for Power* 102(3):305–314.

Ludwig, G. R., and Nenni, J. P. 1980. Tests of an improved rotating stall control system of a J-85 turbojet engine. *ASME 80-GT-17, Journal of Engineering for Power* 102(4):903–911.

Methling, F. O. et al. 2000. The onset of aerodynamic instability in a 3-stage transonic compressor. *NATO/RTO Symposium on Active Control Technology*, May, Braunschweig, Germany.

Murray, R. M. et al. 2001. Compression system dynamics: Control and applications. *VKI/RTO Special Course*, Active Control of Engine Dynamics, 14-18 May, Von Karman Institute for Fluid Dynamics Brussels, Rhode-St-Genese, Belgium.

Paduano, J. D. et al. 2000. Compressor stability and control: Review and practical implications. *NATO/RTO Symposium on Active Control Technology*, May, Braunschweig, Germany.

Regnery, D. 1998. Development of a system for the observation of the stable operation in multistage axial compressors. *VDI-Ber. Nr.1425, 199–210*.

Rippl, A. 1995. Experimentelle untersuchungen zum instationären betriebsverhalten an der stabilitätsgrenze eines mehrstufigen

transsonischen verdichters, dissertation, Ruhr-Universität Bochum.

Ritter, H. et al. 1991. *Neuronale Netze*, Addison Wesley Publishing Company, Bonn, Paris and Reading, MA.

Schulze, R. et al. 1998. Experimental examination of an axial compressor as a basis for an active stall avoidance system. *ISROMAC-7 Paper*, 22–26 February, Honolulu, HI.

Tryfonidis, M. et al. 1994. Pre-stall behaviour of several high-speed compressors. *ASME 94-GT-387*.

Walbaum, M., and Rieß, W. 1998. Einfluß der leitschaufelverstellung auf die entwicklungsformen des rotating stall in mehrstufigen verdichtern. *VDI-Ber. Nr.1425, 177–188*.

Zell, A. 1994. Simulation Neuronaler Netze, Addison Wesley Publishing Company, Bonn, Paris and Reading, MA.